MDPI

Review

Thermal Barrier Coatings for High-Temperature Performance of Nickel-Based Superalloys: A Synthetic Review

Izabela Barwinska [1] , **Mateusz Kopec** [1,]* , **Dominik Kukla** [1] , **Cezary Senderowski** [2]
and Zbigniew L. Kowalewski [1]

1 Institute of Fundamental Technological Research, Polish Academy of Sciences, ul. Pawińskiego 5B, 02-106 Warsaw, Poland; dkukla@ippt.pan.pl (D.K.)

2 Faculty of Mechanical and Industrial Engineering, Warsaw University of Technology, ul. Narbutta 85, 02-524 Warsaw, Poland

* Correspondence: mkopec@ippt.pan.pl

Abstract: With the rising demands of industry to increase the working temperature of gas turbine blades and internal combustion engines, thermal barrier coatings (TBC) were found to be an effective way to further enhance the lifetime of aero components through the improvement of mechanical properties and oxidation-resistance. Thus, this paper aims to review coating technologies with special emphasis on plasma-sprayed thermal barrier coatings (PS), and those produced by physical vapor deposition (PVD) and chemical vapor deposition (CVD) methods. Each technology was assessed in terms of its effectiveness to enhance the mechanical response and oxidation resistance of nickel-based parts working at high temperature. The effect of coating technology on mechanical strength, hardness, fatigue and creep of nickel alloys was discussed to reveal the potential candidates for future applications in aggressive environments.

Keywords: high temperature corrosion; fatigue; creep; aggressive environment; turbine blade

1. Introduction

Nickel-based superalloys are widely used for engine parts since they effectively work under extreme conditions. The main advantages of these materials are their superior heat resistance and high strength, which could be maintained over a wide temperature range [1]. These properties make them particularly attractive materials for aerospace and power engineering applications, including internal combustion engines or gas turbines operated in the air or steam [2]. The recent trends in the power engineering industry require improving the efficiency of these engines by increasing the temperature of the working medium. Such a phenomenon leads to the expansion of the gas in the turbine chamber, thus more energy could be produced [3,4]. However, the combination of high temperature and air to which nickel alloys are exposed leads to their oxidation. Therefore, protective coatings must be applied to increase the material's high-temperature corrosion resistance [5].

These protective coatings are known as thermal barrier coatings (TBC). The research on their particular application to protect turbine blades has continuously developed since the late 1940s. It is important to mention that the still progressing research on TBC is related and driven by both the development of nickel-based superalloys (from casting alloys to directionally solidified alloys and single crystal alloys) and their fabrication methods. The evolution of materials and coatings used for turbine blades was presented in Figure 1 [6,7]. It should be highlighted that a significant improvement in the operating temperature from 900 °C to almost 1500 °C could be obtained by the application of TBC. On the other hand, the increase of working temperature of about 100 °C was observed for nickel-based superalloys manufactured by using different technologies. One can conclude

that application of TBC could improve the high-temperature performance of nickel-based alloys more effectively than the modification of the alloy.
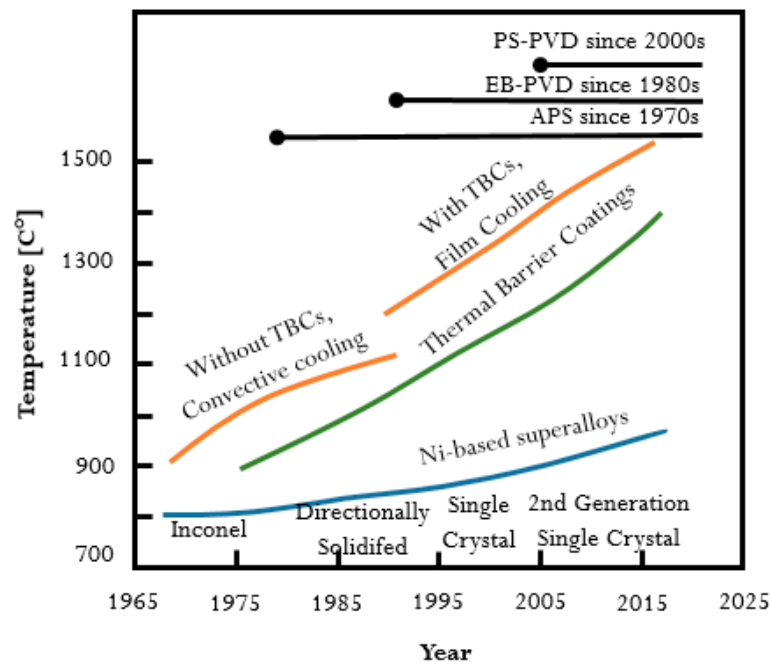

Figure 1. Development of nickel-based superalloys and TBCs over the years in relation to the gas turbine engine operating temperature.

Continuous development of TBC and materials for high-temperature applications require a deep understanding of their mechanical and microstructural properties, especially in relation to their behaviour at elevated temperatures. Although there are a number of review papers found on the TBC deposited on nickel alloys, the effect of coating technology and coating itself on the mechanical response of the substrate material at high temperature and their corrosion resistance was insufficiently discussed. Therefore, the main aim of this paper was to discuss the relationship between coatings and the high-temperature performance (mechanical behaviour and corrosion resistance) of nickel-based alloys.

2. Review Methodology

The literature review involved the detailed investigation of thermal barrier coatings applied on nickel-based superalloys with particular emphasis on their high-temperature performance (mechanical response and oxidation resistance). The review was conducted in the PubMed and Web of Science databases with the following keywords used in various combinations: "thermal barrier coatings, nickel alloys, high temperature performance, fatigue, creep, wear, coatings, oxidation, turbine blades, deposition". A total of 120 scientific papers and conference proceedings were found through the electronic databases. They were subsequently considered by independent reviewers to assess their eligibility. The assessment includes screening the title, abstract and summary of each paper using the pre-specified inclusion and exclusion criteria. In the next step, the papers not fitting the inclusion criteria were excluded. A total number of 98 papers were found as relevant, and thus, they were used in this review.

3. Deposition of TBC Layers

Thermal barrier coatings could be deposited on the material using diffusion or overlay coating processes. During the diffusion process, the protective materials (commonly aluminum and chromium or aluminum and silicon) are evaporated on the hot component (approx. 900 °C) without contact between the substrate material and the powder. However, the powder is in direct contact with the substrate during the overlay coating process.

Despite such a difference, both processes are designed to apply a coating that protects the component against high-temperature corrosion, oxidation and erosion, especially in harsh environments [5,8].

The purpose of a heat insulating coating application is to protect the substrate against high temperatures by inhibiting the transport of heat deep into the material, and thus, extending the life of the component. Specifically, an application of TBC increases the efficiency of turbines by increasing their operating temperature. Additionally, it reduces the proportion of CO_2 and NOx emissions into the atmosphere.

TBCs are typically composed of three layers (Figure 2). The ceramic topcoat is the one of most exposed to high temperatures, thus it is characterized by superior heat resistance, non-conductivity and a low coefficient of thermal expansion. Another important property of the topcoat is its high crack resistance [5,9,10]. The most common material used for the topcoat layer is yttria-stabilised zirconia (YSZ), which has a very high melting point of 2700 °C and one of the lowest thermal conductivities and thermal expansion among conventional ceramic materials [11]. The layer below, called the bond coat, connects the ceramic material with the substrate. The main alloys used for the bond coat are NiCrAlY and NiCoCrAlY. They are characterized by increased corrosion resistance due to their chromium content and improved adhesion related to the addition of the yttrium. One should mention that yttrium, like aluminum, contributes to the inhibition of grain growth, which makes the alumina layer formed at elevated temperatures adherent, continuous and thermally stable [12]. A thin layer of barrier oxides formed between the bond coat and the ceramic topcoat protects the bonding layer from high-temperature oxidation. This layer of thermally grown oxide (TGO) is formed during oxidation of the bond coat and is associated with:

- the formation of microcracks in the topcoat, through which oxygen reacts with the metal to form Al_2O_3 scale; or
- the diffusion of oxygen from the YSZ decomposition.

Despite the high-temperature corrosion resistance of the alumina oxide and beneficial effects leading from the addition of Y, many contradictions can also be found in the literature. They demonstrate the negative effect of such an addition on the long service life of the coating [13]. The effect of the Y addition in the coating on oxidation was studied by et al. Hu [12], who performed detailed microstructural studies on oxidized TBC, paying particular attention to the YSZ/NiCrAlY interface region. Isothermal oxidation testing in the air at 1050 °C for 24, 96 and 192 h were performed on Ni-based superalloy GH3030 specimens with YSZ coating applied by the APS technique. The result showed that the YAG layer formed on the Al_2O_3 layer after high temperatures oxidation leads to a reduction of the service life of the TBC. Such behaviour was related to the reduction of Al_2O_3 layer thickness and subsequent acceleration of the outward diffusion of Ni and Cr elements [9,14].

One should highlight that almost 98% of alloys and superalloys capable of operations above 700 °C in an oxygen environment contain as high as 18 wt.% of Cr and less than 2 wt.% Al. Chromium-rich alloys usually form Cr_2O_3 oxide during air or oxygen exposure, and thus, the dissociation of Cr_2O_3 to CrO_3 limits their oxidation resistance to 950 °C [15]. Therefore, a special group consisting of nickel and iron aluminides possessing a high melting point, low density, excellent high-temperature endurance, and corrosion resistance above 950 °C was developed [15,16]. Iron and nickel aluminide-based alloys (Ni_3Al, NiAl, Fe_3Al and FeAl) exhibit superior resistance to high-temperature corrosion in the aggressive environment due to the formation of a protective alumina layer, even when the partial pressure of oxygen is low. Among these materials, iron aluminides based on Fe_3Al and FeAl exhibit attractive properties in comparison to steels and superalloys as indicated below [17–22]:

- lower density than stainless steels, and better strength-to-weight ratio;
- higher Al content (in the range of 15–30 wt.% depending on the intermetallic) as compared to Al content of 6 wt.% or less in steels and superalloys;
- excellent oxidation resistance up to 1000 °C;
- better corrosion resistance in oxidizing and reducing environments;
- the ability to either reduce or eliminate the application of strategic elements such as Cr;
- the ability to match thermal expansion properties with those of the steels;
- high electrical resistivity that increases with temperature;
- good corrosion resistance in many aqueous environments.

Reinshagen et al. [23] obtained Fe_3Al-based coatings by spraying 5.5–62 μm size gas atomized powder of Fe-15.9 wt.% Al-2.2Cr-0.01B onto the Inconel 718 substrate using APS and HVOF techniques. Interestingly, coatings of HVOF exhibited low porosity, a high number of partially unmelted particles and a stable connection, whereas a large amount of intersplat porosity with low adhesion was observed for APS coatings. Al-Taie et al. [24] investigated the potential use of Fe_3Al-based coatings for corrosion and erosion resistance in coal gasification systems by application of Fe_3Al-based coatings on 800H, 304, Sanicro 28 and Monit substrates. Interestingly, Fe_3Al coatings exhibited limited corrosion even after 1500 h exposure at 600 °C in a CO-30%H_2-3.5%H_2O-1.5%H_2S atmosphere despite spallation of the coatings from the substrates. Spallation is a serious concern and requires either modification of the substrate prior to application of the coating or deposition of an intermediate bond coating. Senderowski et al. [25] applied NiAl and NiCr interlayers for GDS Fe-Al intermetallic coatings obtained from self-decomposing powders. The successful application of a coating system enabled to enhance mechanical and thermal resistance above 950 °C, hardness and the adhesion of the coating/substrate bond. Deevi [15] shown that HVOF and APS protective Fe_3Al- and FeAl-based coatings exhibit excellent oxidation and corrosion resistance in air and in complex corrosive environments such as H_2-H_2S, N_2-11.2$O_{2-7.5}$$CO_2$ with SO_2, O/S mixed-gas environments with or without chlorine, sulfur, molten salts and condensed alkali deposits in the temperature range of 700–1100 °C for extended periods of time.
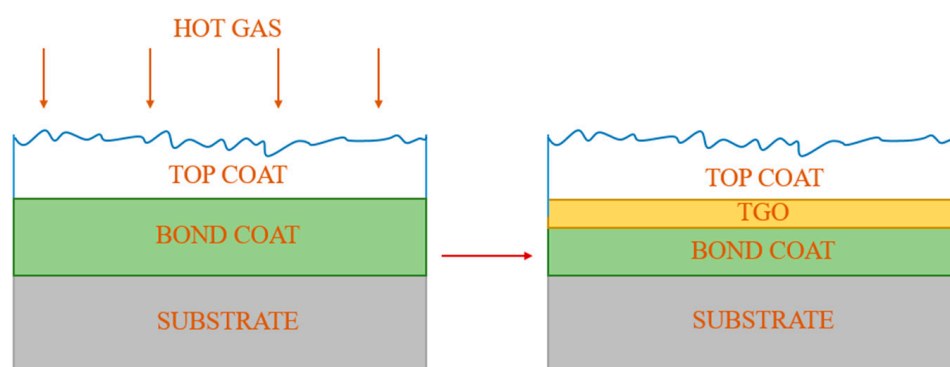

Figure 2. Schematic of TBC system formation.

Typically, TBCs also consist of a bilayer material system that involves a bond coat (BC) and a ceramic topcoat (TC). TCs are commonly deposited by using atmospheric plasma spray (APS) and electron beam vapor deposition (EB-PVD) methods. Other techniques include suspension plasma spray (SPS) and plasma spray–physical vapor deposition (PS–PVD) which form a coating with a columnar microstructure similar to EB-PVD, however, at a considerably lower cost [26]. On the other hand, the BC could be applied by using all the plasma spraying processing methods including air, vacuum and low-pressure (APS, VPS and VLPPS) methods, as well as high-velocity oxy-fuel (HVOF) and chemical vapor deposition (CVD) [27].

3.1. Thermal Sprayed Methods

Thermal spraying is a process during which a material, usually with a high melting point, is applied to a component using a plasma jet or supersonic flow of a gas stream in the HVOF or DGS (D-gun spraying) methods. The plasma or energy-carried medium is used to heat or melt the feedstock material, which is subsequently injected into the plasma in the form of a powder, rod or wire. The high pressure and velocity of the heated feedstock cause particle droplets to flatten upon impact and build up subsequent layers of droplets (Figure 3). The coatings obtained during such process are characterized by a layered structure. In this structure, interlayer pores formed during rapid solidification and uneven sputtering can usually be observed. The uniform distribution of voids between the particles is very important during the application of ceramic coatings, as they reduce the flow of heat flux to the bonding layer and the component [28–31]. In addition, this microstructure enables the introduction of more scattering centres, which effectively diminish the amount of radiative heat build-up on processed components, such as gas turbines [32]. This coating process was found to be excellent for large-area components, since the deposition is performed at high speed and with considerable efficiency [33]. Depending on the specific gas atmosphere, the PS process could be classified into several variants:

- atmospheric plasma spraying (APS) carried out in a controlled air atmosphere;
- low-pressure plasma spraying/vacuum plasma spraying (LPPS/VPS) performed under controlled vacuum (at pressures of 3–7 kPa);
- very low-pressure plasma spraying (VLPPS), which is also performed under a controlled vacuum within the pressure range from 50 Pa to 200 Pa [30];
- suspension plasma spray (SPS) and solution precursor plasma spray (SPPS) processes [31] in which the coating material is delivered into the plasma jet as suspended solid particles in a nanometer or micron size range (in the SPS process) or an aqueous or non-aqueous solution (which is fed into the plasma) containing the cations necessary to form the oxide coating (in the SPPS process).
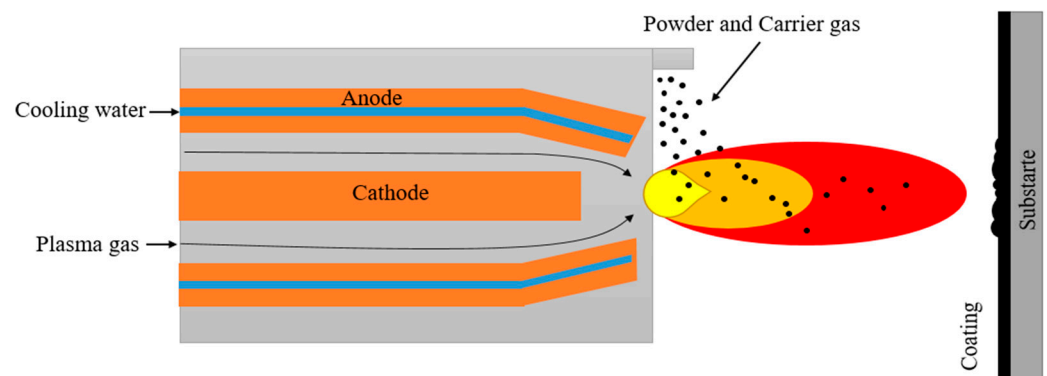

Figure 3. Schematic process of coating deposition by using thermal spray method.

A relatively new method among thermal spray coating techniques is the high-velocity oxygen fuel (HVOF) method, which, in contrast to the previous methods, uses a supersonic jet for the powder atomization. The supersonic velocity (above 1000 m/s) of the gas passing through the converging/diverging nozzle is created by the combustion of a mixture of liquid or gaseous fuel (propane, acetylene, propylene, hydrogen, kerosene) with oxygen in the chamber. Depending on the oxygen and fuel ratio, the gas stream has a different pressure and temperature between 2500–3100 °C. Such conditions enable the powder material to be heated to its molten state and notably increase its speed towards the substrate [32,33]. The higher velocity of the particles improves the properties of the coatings, since shorter transit time reduces the formation of oxides on the one hand and reduces porosity to less than 1% on the other [33,34].

Slightly different from HVOF technology is the D-gun spraying method (DGS), which enables us to obtain much higher particle velocities than HVOF [35,36]. Contrary to known HVOF–HVAS-type thermal spraying techniques, the detonation spraying procedure is characterized by a much higher complexity of the thermophysical detonation phenomena [35,36]. It is related to the unstable gas flow conditions with high temperature and pressure gradients and high rates of local temporal DGS parameters change during the gas detonation process with a specific frequency. D-gun-sprayed coatings exhibit excellent adhesion to the substrate with very low structure porosity [37,38].

3.2. Vapor Deposition Techniques

TBC can also be produced by using vapor deposition techniques. These methods are used to fabricate thin layers with thicknesses ranging from a few nanometers to several hundred microns. Technologies for producing coatings using gas-phase deposition techniques can be classified into physical vapor deposition (PVD) and chemical vapor deposition (CVD) [39]. The main advantage of these coatings is that they can be applied on a variety of complex-shaped objects (insides and undersides of features, elements with holes, etc.) [40–43].

PVD is a deposition process in which a material is sublimated or evaporated under heat into atoms or molecules, and transported to a substrate where it is condensed atom by atom (Figure 4). The deposition chamber is kept either under low pressure gas (or plasma) or a vacuum. It enables the particles to move towards the substrate (usually following a straight path) and reduces gaseous contamination [44].
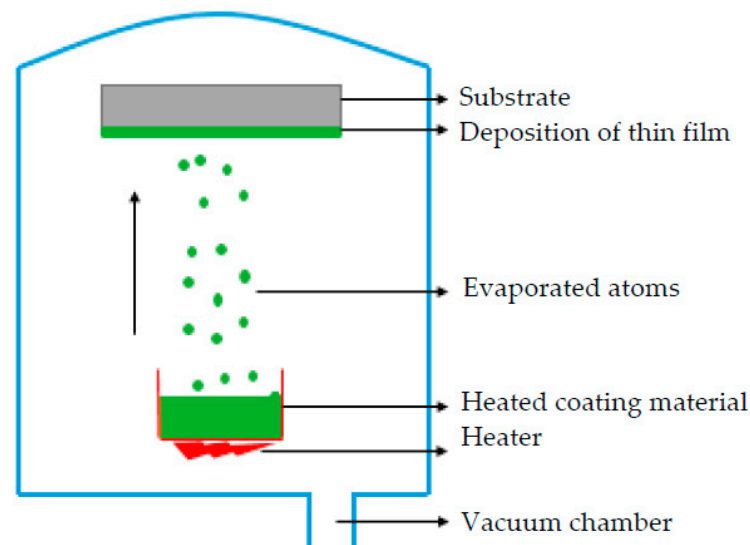

Figure 4. Schematic process of coating deposition by using PVD method.

Among a number of PVD processes, EB-PVD is one of the most commonly used in the industry. In this method, the target material is bombarded and melted by an electron beam, vaporized and subsequently deposited on the surface, resulting in a unique columnar microstructure formation [45]. Columnar grains are aligned perpendicularly to the substrate and demonstrate the ability to stress accommodation, enhancing thermal-shock resistance during part performance. TBC coatings produced by the EB-PVD process are more frequently deposited on components for the most difficult applications, such as turbine blades in aircraft engines [46,47]. However, the main disadvantage of this process is that thermal conduction paths occur between the columns, which increases the thermal conductivity of the coating. Furthermore, it is also considered the most expensive and complex industrial coating process [48,49] with a significantly lower deposition rate of the coating deposition [50].

CVD is another widely used diffusion method for the deposition of thin films in which material in the vapor phase is deposited on the heated substrate surface. In a typical CVD process, one or more volatile precursors are located in the chamber, where they react with each other and/or decompose on the surface to form a layer of a single material. Usually, some components of the gas undergo chemical decomposition during interaction with the substrate, forming volatile by-products that are pumped out of the reaction chamber (Figure 5a) [51]. The advantage of this method over PVD is the possibility of depositing a large variety of materials at relatively low temperature (500–1000 °C) and atmospheric pressure (10 mbar). The deposited coatings are homogeneous and exhibit high purity [52]. A typical example of morphology showing the coating obtained during CVD process was presented in Figure 5b, while its cross section was shown in Figure 5c. The deposition process was performed at a temperature of 950 °C for 4 h on MAR 247 as a substrate material.
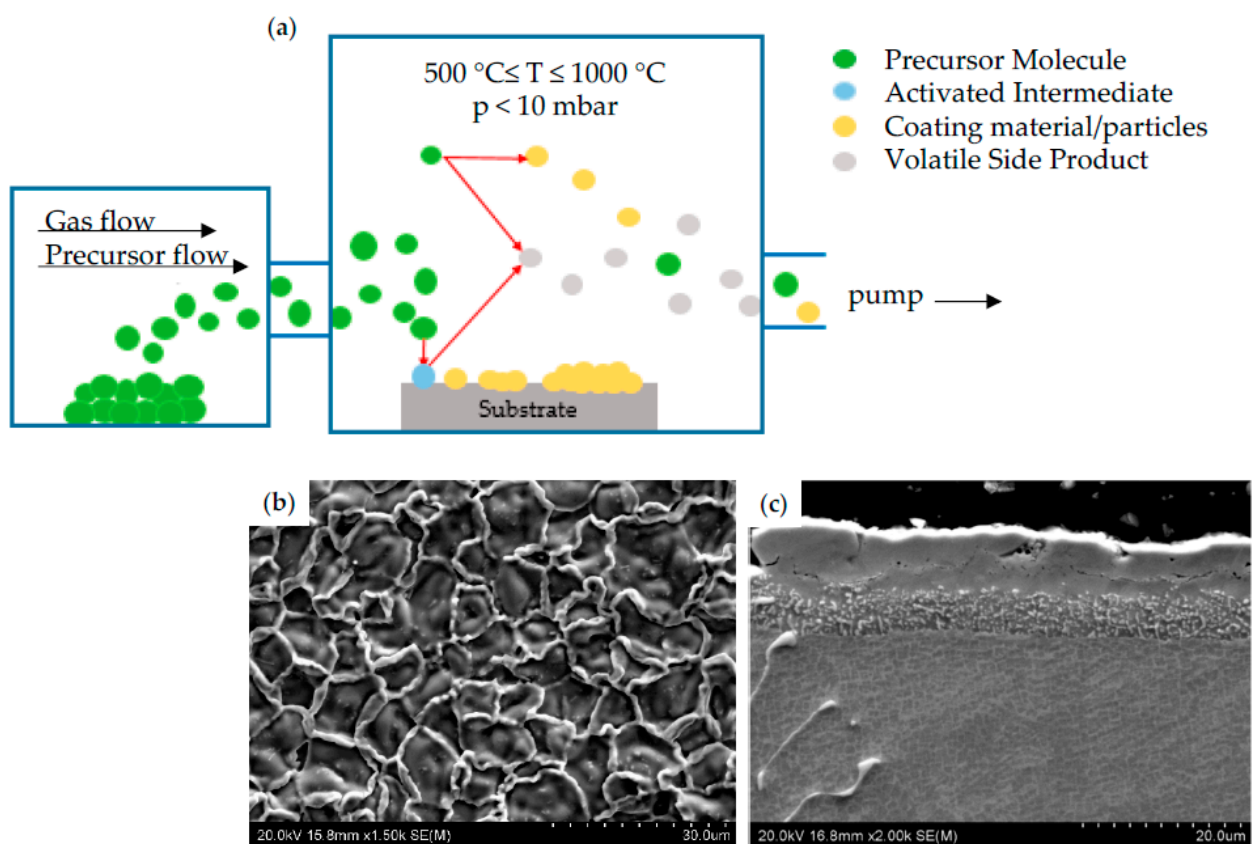

Figure 5. Schematic process of coating deposition by using CVD method (**a**); morphology (**b**) and cross-section (**c**) of CVD coating.

3.3. Perspective Methods—Physical Vapor Deposition (PS-PVD), Suspension Plasma Spray (SPS)

Another evolving technique combining the advantages of APS and EB-PVD methods is plasma spray–physical vapor deposition (PS–PVD). This promising technology was developed to achieve conditions that were unattainable for the two methods mentioned above. First of all, PS–PVD has the ability to deposit columnar structure coatings such as EB-PVD; however, this is completed by using thermal spray technology, during which the material is evaporated. Evaporation of the feed material was achieved by reducing the working pressure. It results in a change of the plasma plume properties and increases the energy of the plasma (temperature up to 10,000 °C). Additionally, PS–PVD coatings, as well as those produced by APS, exhibit porosity, which is not possible to obtain with the EB-PVD method. Mentioned properties are favourable for the achievement of high in-plane strain tolerance with low thermal conductivities [53,54].

The second alternative method is suspension plasma spray (SPS), which enables us to manufacture of columnar structures. The difference between APS is mainly related to the size of injected particles during the process. Suspension plasma spray process used nano or submicron-sized powder feedstocks and a liquid medium. In contrast, APS cannot use particles with diameters lower than 5 μm [49]. The ability to deposit the fine particles provides higher thermal mechanical properties as compared to micron-sized powders [55]. Thus, during the SPS small particles are deposited by using liquid (water or alcohol) in which the particles are suspended. The suspension is injected by the nozzle, and then penetrates through the plasma jet with adequate velocity. Subsequently, the suspension is fragmented during the transport, the solvent is vaporized, and the particles are melted and finally deposited on the substrate [56].

In the SPPS process, a precursor with a high molar concentration is used. However, it should be highlighted that it is challenging to find the stable precursor solutions from soluble and mutually compatible chemicals in a given solvent. Typically, the various steps of SPPS coating formation include droplet breaking, solvent evaporation, particle pyrolysis, melting, and finally, deposition could be distinguished. A unique feature of the SPPS process is that chemical precursors can exhibit endothermic or exothermic chemical reactions, or a combination of both, during pyrolysis. The specific energy of these reactions is often sufficiently high to accelerate particle decomposition and melting. Therefore, the use of specific features of the SPPS process, such as the occurrence of exothermic reactions, enable us to obtain unique microstructure in TBCs coatings, including metastable phases and homogeneous two-phase structures.

4. Effect of Deposition Methods on Corrosion Resistance and Mechanical Properties

Since coated nickel superalloys operate mainly at high-temperature and high-pressure environments for a long period of time, several tests have been conducted to verify their oxidation resistance and mechanical response under such aggressive conditions. These properties are mainly affected by the structure, which can be classified into columnar and lamellar depending on the method used. Moreover, the parameters applied during the process (size of powder, spray distance, spray rate, current value, etc.) also have a significant effect on the coating's microstructure. Hence, they should be carefully controlled during deposition [57].

4.1. Effect of TBC on Corrosion Resistance

Failure of TBC exposed to high temperature is commonly associated with the growth of TGO due to BC oxidation. Such growth causes the occurrence of additional stress acceleration of the nucleation, growth and propagation of microcracks between layers or in the TGO layer. Thus, controlling the formation and thickness of TGO is one of the key factors in the determination of the TBCs lifetime and durability [46]. The cross-section view of NiAl coating obtained during CVD process on Inconel 740 (Figure 6a) and subjected to high temperature at 1000 °C for 1 h and 25 h in air are presented in Figures 6b and 6c, respectively.
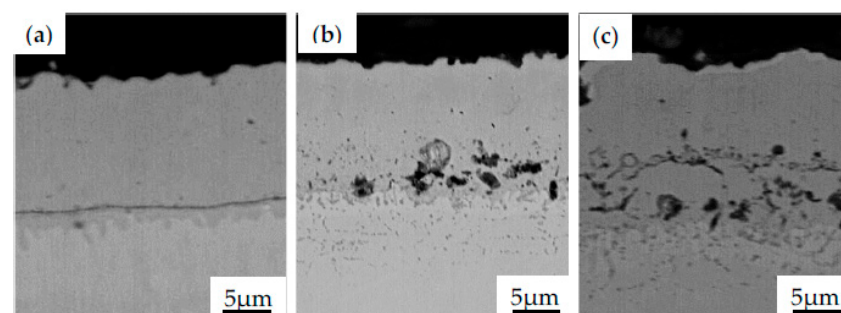

Figure 6. The microstructural evolution of the NiAl coating obtained during CVD process in the as-received state (**a**) and subjected to high temperature at 1000 °C for 1 h (**b**) and 25 h (**c**).

One could observe the growth of oxides and microvoids between substrate material and coating resulting from the mentioned bond coat oxidation. Similar micro-cracks have been observed in pure nickel plates aluminized in an Ar atmosphere by using a halide-activated pack-cementation in a powder mixture of Al + 55 wt.% Al_2O_3 + 5 wt.% NH_4Cl [58]. It was reported that, after 5 h of high temperature exposure in the air at 1000 °C, microcracks on the topcoat were observed. These cracks were related to the compressive stress found in the coating. Such a type of stress originates from the oxide volume contraction converted during the transformation of the θ-Al_2O_3 phase to α-Al_2O_3. Doleker et al. [59] reported cracking and columnar spallation on the YSZ/$Gd_2Zr_2O_7$ ceramics coating deposited on Inconel 718 by using the EB-PVD method. The effect of oxidation on as-received and coated specimens was examined at 1000 °C for 8, 24 and 100 h in the ambient atmosphere. The dominant phase found in oxidized Inconel 718 was Cr_2O_3, with internal oxidation and thickness of the oxidation increasing in time. However, after the 100-h oxidation test, the stresses induced by the formation of NiO, TiO_2, $CrNbO_4$, $TiNb_2O_7$, $CrMoO_4$ and their thermal expansion led to the cracking along the interface of the topcoat. Nevertheless, it was concluded that the application of the ceramic coating layer provides higher oxidation resistance by hindering oxygen penetration into the material as compared with the as-received Inconel 718. Similar observations were performed by Barwinska who investigated the oxidation of Inconel 740 alloy coated with NiAl. It was found that after exposure for 100 h at 1000 °C, the coated alloy exhibited microstructural changes in depth of 35 µm (Figure 7a), while the as-received alloy was oxidized for up to 80 µm (Figure 7b). Such results clearly indicate that the protective layer effectively protects Inconel 740 against hot corrosion.
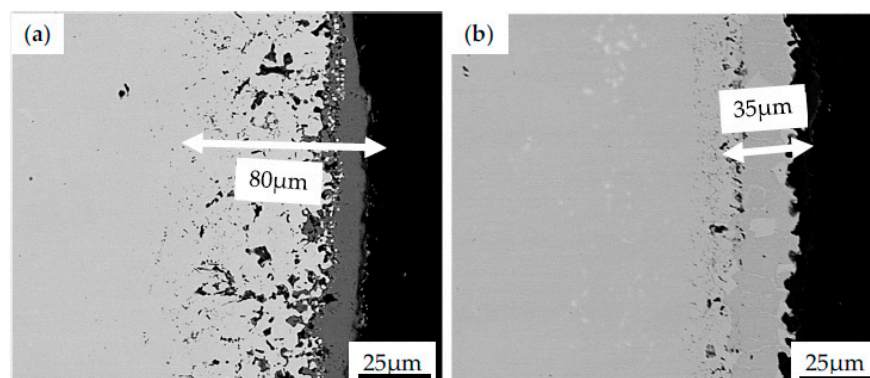

Figure 7. The surface evolution of Inconel 740 in the as-received state (**a**) and with the NiAl coating obtained during CVD process (**b**) after exposure to high temperature at 1000 °C for 100 h.

The TBCs also spall due to the coefficient of thermal expansion (CTE) mismatch between metals/alloys and ceramics upon cooling to ambient temperature. One should highlight that it is important to combine materials with similar thermal expansion coefficients to reduce tensile stress generation and further avoid coating cracking [60]. Several studies have been performed to assess a suitable sprayed MCrAlY bond coat [61–63] that could potentially enhance the high-temperature performance of nickel-based alloys, however, with limited success. The durable TBC coating over long thermal cycles was developed by He et al. [60], who used advanced MCrAlY alloys applied on Hastelloy-X. In this research, five different materials (AE11964, AE11965, AE11966, Diamalloy 4700 and Amdy 386) were deposited on the substrate as the bond coat by using HVOF/DJ 2600 method. Additionally, the 7YSZ topcoat was applied by using the air plasma (Sinplex) sprayed method. The coatings of 300 µm thickness were heat-treated under vacuum for 4 h at 1080 °C. Subsequently, furnace cycle testing (FCT) was carried out at 1135, 1155 and 1165 °C. The specimens were heated up to the testing temperature for 10 min, then annealed for 50 min, and subsequently, cooled for 10 min by air quenching. The results showed that all alloys have higher thermal cycle properties than benchmarking alloy D4700. Significant

improvement was observed for AE11966, where thermal cycle resistance increased by 248% at 1135 °C and 158% at 1165 °C, as compared to D4700. It was highlighted that the higher temperature of tests reduced TBC lifetime 5-fold for every 100 °C. The excellent FCT performance was related to the fact that AE11964, AE11965 and AE11966 bond coats were characterized by more than 50% less thermal expansion below 800 °C between the topcoat and a slower TGO growth rate. Different results were presented by Wells et al. [64], who have shown how the APS thermal barrier coating influences the oxidation resistance of nickel alloys. The curved specimens of Inconel 6203 were protected by using two coatings: LPPS CoNiCrAlY bond coat and an APS 8 wt.% YSZ topcoat. One of the specimens was edged with a radius of 1.5 mm, while the other with 0.35 mm. Such curvatures were chosen to simulate the corrosion process that occurs on blade rounding. Subsequently, specimens were subjected to continuous isothermal heating at 850 °C for 1000 h and cyclic oxidation at 900 °C for 1 h, followed by air cooling. The observation of specimens' surface after the testing showed that small radii may contribute to a more rapid hot corrosion process, potentially as a result of increased scale spallation. Furthermore, the specimens exposed to isothermal process were characterized by thinner TGO than those after the cyclic oxidation. Despite a thinner TGO, delamination cracks on TBC were observed under such conditions, which were not evident on the specimens after cyclic process. On the other hand, the thicker areas of TGO with potentially more mixed oxides may have created localized high stress regions to cause delamination cracks. The effect of the APS topcoat application on the oxidation resistance of the Haynes 230 was also performed during the cycle oxidation test every 100 h at 850 °C for 1000 h on the three different specimens: without APS topcoat, with APS topcoat and with damaged APS topcoat [64]. Specimens were also covered by LPPS bond coat. The test was performed in a corrosive environment of 0.7 vol% SO_2, 14.6 vol% O_2 and N_2 and with a $Na_2SO_4:K_2SO_4$ applied to the surface of specimens every 100 h. The results showed that TBC reduced the hot corrosion of the alloy significantly. The observed TGO was thinner and more stable, even where the TBC had been pre-cracked, than in the specimens with no topcoat. The effect of corrosion atmosphere could be clearly observed in Figure 8, in which the images of morphology of MAR247 with NiAl coating obtained during CVD process in the as-received state (Figure 8a), after being subjected to high temperature corrosion test at 1000 °C for 100 h (Figure 8b) and after corrosion test in 0.3 M NaCl solution (Figure 8c) are presented.

The as-received coating after deposition process was characterized by a large number of craters with a relatively smooth surface. The high temperature exposure led to the formation of needle-like features on it. On the other hand, the corrosive environment of 0.3 M NaCl solution resulted in the growth of alumina-based crystals.
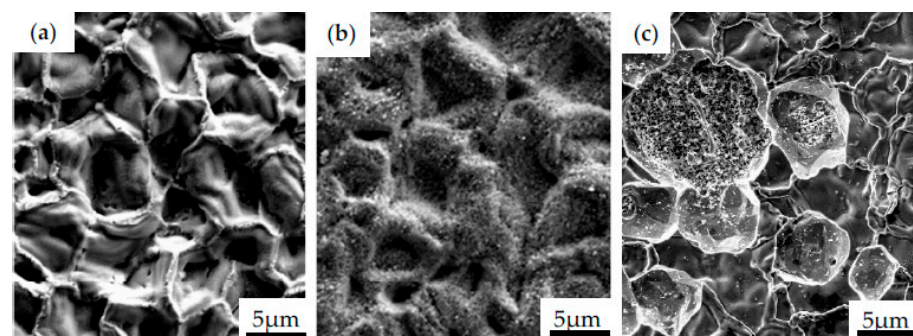
Figure 8. The images of morphology of MAR247 with NiAl coating obtained during CVD process in the as-received state (**a**), after high temperature corrosion test at 1000 °C for 100 h (**b**), and after corrosion test in 0.3 M NaCl solution (**c**).

Similarly, the influence of different bond coats in SPS TBCs on a lifetime of Hastelloy-X and Inconel 792 was examined by Gupta et al. [65]. In this work, NiCoCrAlY bond coats prepared by HVAF and VPS were compared to PtAl diffusion bond coat. Specimens were

covered with a YSZ topcoat by using the SPS method; however, some of them were grit-blasted before the deposition. The microstructure observation showed that even though all specimens were covered with the same SPS parameters, the formed columns in the topcoat were thinner than in others, resembling an EB-PVD coating. This phenomenon has been observed due to the characteristic lower surface roughness of the diffusion layer. It provides higher adherence of large particles during deposition in the first few layers to further create more initiation peaks, as reported in the literature [66–68]. However, due to the poor mechanical bonding between SPS topcoat and a smooth bond coat surface, spallation frequently occurs during metallography preparation for microscopic observations. Such a low adhesion also affects the formation of spallation during the isothermal heat treatment test at 1100 °C. The selected images of cracked coating observed after preparation of the metallographic specimen are presented in Figure 9a. One should highlight that the TBC layer have a fragile nature, so they crack easily when subjected to excessive loading. However, if the optimized parameters of deposition process are selected, the coating is well-adhered to the substrate. Figure 9b shows the fracture area of the Inconel 740 with NiAl coating subjected to cyclic loading at room temperature. It should be noticed that even if the surface cracks appear, the coating remains on the substrate, which may confirm the effectiveness of the process parameters applied.
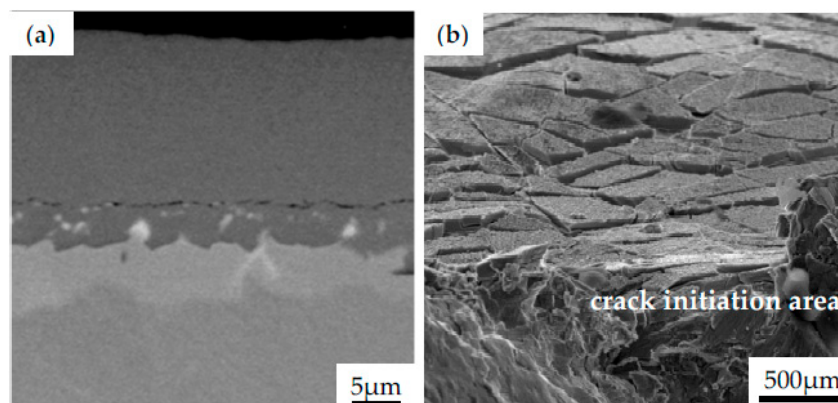

Figure 9. The morphology of Inconel 740 with NiAl coating obtained during CVD process after preparation of metallographic specimen (**a**), top view of the NiAl coating after fracture of the specimen subjected to cyclic loading (**b**).

On the other hand, both HVAF and diffusion bond coat form a thin, dense and uniform TGO layer after 200 h of high temperature exposure [65]. Such slow growing TGO layer is typically desired, since it could prevent excessive oxidation. Moreover, it could potentially lead to the increase of high internal stress. Moreover, the uniform and thin alumina layer was responsible for exhibiting the highest TFC resistance in the diffusion layer. In comparison to the HVAF and VPS after TFC testing, it was observed that the HVAF bond coat was characterized by around 20% higher TCF lifetime than VPS. However, in both cases, no significant improvement in TCF service life was found after the application of grit-blasted bond coats. Similar observation was reported by Kumar et al. [26] who have identified and distinguished the properties of columnar TBC produced by different processes. In this study, nine different sets of TBCs were investigated to optimize the manufacturing process that will further enable us to obtain ideal columnar microstructure, which exhibits a combination of relatively low thermal conductivity and improved lifetime. The TFC tests also exposed that all specimens of HVAF BC were characterized by longer lifetimes than those of VPS BC. Moreover, in comparison to APS, SPS and PS–PVD TC in different configurations (standard, porous and dense), dense PS–PVD coating was proven to be the most durable in terms of thermal cyclic fatigue and burner rig resistance. Based on the results and existing knowledge, a theoretically ideal TC columnar microstructure concerning column density, intracolumnar porosity and intercolumnar gap was proposed. It

was reported that such an ideal columnar microstructure should offer a high column density similar to PS–PVD and EB-PVD coatings. Moreover, it should have narrow intercolumnar gaps improving their strain tolerance and the desired features in this structure would be medium intracolumnar porosity, resulting in lower thermal conductivity. A quality of the coating is influenced by the structure, which depends mainly on the method used. It is also related to the process parameters, among which the most important is the powder particle size. Interesting studies showing the dependence of the oxidation resistance on the particle size used during the VPS deposition process were carried out by Seo et al. [69]. It was reported that particle size significantly influences statistic oxidation. CoNiCrAlY and CoCrAlY powders with various particle size ranges were deposited on Inconel 718 substrates as coatings. In order to identify oxidation behaviour, isothermal oxidation experiments at 1000 °C up to 1000 h under air conditions were performed. Co-series coatings were characterised by higher weight gain and thickness of TGO than CoNi ones. However, smaller particle sizes of powder produce a relatively smooth surface that enables the formation of a continuous alumina layer. It prevents the rapid growth of TGO by blocking the diffusion process. The summary of the oxidation behavior in relation to the deposition method was presented in Table 1.

Table 1. Summary of the oxidation performance depending on the deposition method applied.

Deposition Method/Substrate	Oxidation-Related Behavior/Main Finding	Ref.
pack-cementation in a powder mixture of Al + 55 wt.% Al_2O_3 + 5 wt.% NH_4Cl/pure nickel	- appearance of cracks after 5 h air exposure at 1000 °C due to compressive stress in the coating; - stress originates from the oxide volume contraction converted during the transformation of the θ-Al_2O_3 phase to α-Al_2O_3	[58]
EB-PVD/Inconel 718	- oxidation on the as-received and coated specimens was examined at 1000 °C for 8, 24 and 100 h in the ambient atmosphere; - cracking and columnar spallation on the YSZ/$Gd_2Zr_2O_7$ ceramics coating due to formation of NiO, TiO_2, $CrNbO_4$, $TiNb_2O_7$, $CrMoO_4$ and their thermal expansion.	[59]
HVOF/Hastelloy-X	- furnace cycle testing (FCT) was carried out at 1135 °C, 1155 °C and 1165 °C; - thermal cycle resistance increased by 248% at 1135 °C and 158% at 1165 °C.	[60]
APS/Inconel 6203	- continuous isothermal heating at 850 °C for 1000 h; - cyclic oxidation at 900 °C for 1 h, followed by air cooling; - the specimens exposed to isothermal process were characterized by thinner TGO than those after the cyclic oxidation; however, the delamination cracks were observed.	[64]
APS/Haynes 230	- cycle oxidation test every 100 h at 850 °C for 1000 h; - a corrosive environment of 0.7 vol% SO_2, 14.6 vol% O_2 and N_2 and with a Na_2SO_4:K_2SO_4 applied to the surface of specimens every 100 h; - TBC reduced the hot corrosion of the alloy significantly.	[64]
HVAF/Hastelloy X and Inconel 792	- formation of dense and uniform TGO layer after 200 h of high temperature exposure.	[65]
VPS/Inconel 718	- CoNiCrAlY and CoCrAlY powders with various particle size ranges were deposited; - isothermal oxidation experiments at 1000 °C up to 1000 h under air conditions were performed.	[69]

4.2. Effect of TBC on Mechanical Properties

The TBC is a combination of multiple materials, which are characterized by different thermo-mechanical properties. Therefore, it is problematic to manufacture a defect-free coating that could withstand a very high temperature and be durable enough to ensure thousands of safe take-offs and landings of the plane engines within the operational time of up to 30,000 h. The thermo-mechanical interactions that occurred in the TBC during their exploitation make them more unpredictable in terms of physical behaviour as compared to any other components made of metal or ceramic [70]. The main factor impacting TBC lifetime is their fracture toughness. The initiation of a fracture in brittle materials subjected to thermomechanical loading is often caused by the presence of manufacturing or processing defects such as pores, cavities, cracks, etc. [71]. On the other hand, both pores and controlled artificially introduced vertical cracks also increase the durability of TBC [72,73]. Porosity is an inherent feature of coatings that reduces thermal conductivity of the TC leading to an increase in the thermal fatigue life of the coated material. However, excessive pore formation affects adhesion significantly and decreases the Young's modulus [74]. In the case of cracks, the properly introduced vertical cracks during the manufacturing process can significantly lower the stress concentration during TGO layer formation. The thicker coating also provides greater thermal barrier performance and minimizes thermal stress, although in aggressive environments the thick coating can lead to faster degradation of coated components [75].

Besides manufacturing defects that accelerate total failure, coated parts are also exposed to complex mechanical loading at high temperature. Continuously increasing demands of the contemporary industry enforce the reduction of the components' weight and maximization of their high-temperature performance. Such combination frequently leads to the induction of high stress levels, that are close to the fatigue limit. Thus, it is extremely important to understand how coating affects the fatigue behaviour of the component [76]. Ray et al. [77] presented that the fatigue limits of C-263 Ni-base superalloy with TBC at 800 °C highly depend on the stress applied. It was reported [77] that lower stress generated higher fatigue limits for coated material than those obtained for the as-received alloy. However, the opposite results were captured for higher stress. Such behavior was related to pores or microcracks formed in the YSZ topcoat since they propagated rapidly in the $Ni_{22}Co_{17}Cr_{12.5}Al_{0.6}Y$ metallic bond coat into the substrate under high stress. The reason for the reduced endurance limit of the substrate material at lower stress was associated with oxidation of the coating surface. On the other hand, Ray et al. [78] indicates that the durability of C-263 Ni-base superalloy coated with $YSZ/Ni_{22}Co_{17}Cr_{12.5}Al_{0.6}Y$ under accelerated creep conditions at temperature 550–800 °C is significantly higher than that of the base material. Since the substrate material possesses relatively low rupture strength at high temperature, the application of TBC will not enhance it properties either. It was concluded that the TBC-coated material should not be used for more than 1000 h under continuous operation at 800 °C, as its strength drastically decreases. Dong et al. [79] observed a completely different dependence during the fatigue testing of the DD6 single crystal superalloy with NiCoCrAlYHf BC deposited by the arc ion plating and zirconia-based EB-PVD TC in which the TBC-coated alloy exhibited higher fatigue limits under high stress at 900 °C. It was found that two factors are responsible for the fatigue life improvement. The first one is related to the fact that the coating can transfer a part of the load. The second one is associated with the residual stress which is formed between the layers during deposition. In addition, the fatigue life of the coated alloy decreases with decreasing stress, which may be influenced by the mutual interdiffusion between the layers. Since high temperature exposure accelerates the growth of TGO, a simultaneous reduction of outer layer thickness could be observed. Additionally, the interdiffusion process can also determine materials properties due to excessive transition of the strengthening elements to the bond coat. Interdiffusion could also lead to the formation of pores and other defects between the substrate and BC, which may cause more rapid failure through spallation when subjected to load. Kopec et al. [80] also reported that the NiAl coating deposited on MAR

247 nickel-based superalloy by using CVD process increases fatigue response of the base material at 900 °C. It was found that coated material has almost twice the higher strength at 900 °C. Additionally, the creep tests at 600 °C in the air atmosphere also demonstrated that aluminized layer enhances the strength of the MAR 247 by approximately 50 MPa after 500 h of high temperature exposure.

The durability of coating deposited on the material is also frequently assessed through a bending test during which modulus of elasticity and fracture toughness are calculated [81]. Zhu et al. [82] proposed a three-point bending test supported by digital image correlation (DIC) for determination of the critical adhesion energy of the TBC deposited on GH4169 superalloy. It was reported that such an experimental approach could be effectively used for the coating quality assessment. In another research study by Zhu et al. [82], the modulus of elasticity and fracture toughness were determined on the GH536 nickel alloy specimens with TBC (NiCoCrAlY BC and 8YSZ TC prepared by air plasma spraying) by using a high temperature three-point bending test combined with DIC system. The tests were performed at temperatures equal to 30 °C, 400 °C, 600 °C and 800 °C. The results showed that TC elastic modulus gradually decrease with the increase of the temperature. Furthermore, no significant differences were observed between coated and uncoated materials in terms of the loads and the slopes of load-deflection curves obtained. Since the test was monitored by DIC, the critical stress of crack propagation was determined, and subsequently, fracture toughness was calculated. It was found that the fracture toughness of TC decreases from 1.31 MPa m$^{1/2}$ to 1.16 MPa m$^{1/2}$ with temperature increase from 30 °C to 800 °C.

In order to prevent premature damage caused by interfacial delamination between BC and TC, it is also important to understand the anisotropic properties of TBC. The main reason for TBC fracture is local out-of-plane tensile strain energy between these layers. Thus, it is important to study the anisotropy of mechanical properties that include the Young's modulus and fracture strength (e.g., strain of fracture and toughness) [83]. Chen et al. [84] investigated in-plane and out-of-plane modulus and fracture toughness of the APS TBC (NiCoCrAlY-BC and 8YSZ TC) deposited on the Hastelloy X superalloy substrate. Specimens were cut by using a focused ion beam (FIB) on a polished surface of the TBC in two orientations: longitudinal and transverse. The mechanical properties were assessed by using micro-cantilever bending, which revealed that the APS TBC was elastically anisotropic at the microscale. The variation between in-plane and out-of-plane modulus of elasticity was 31%. It was attributed to the dissimilarity of the microstructures in the different orientations and the occurrence of defects and their density. Similar bending tests were performed by Yamazaki et al. [85] on the TBC on the IN738LC substrate prepared by using two techniques. The CoNiCrAlY bond coat was prepared by using HVOF method, while the 8YSZ topcoat with alcohol solvent was deposited by using SPS method. The out-of-plane Young's modulus and shear strength were also determined by using cantilever bending tests. Tests were conducted on the single column of the SPS before and after thermal ageing at 1000 °C for 300 h. The load-displacement curves captured from the shear test showed that the applied load value decreased before a single column crack. In order to compare Young's modulus out-of-plane and in-plane orientations, the researchers conducted a three-point bending test. The results showed that SPS TBCs possess higher anisotropy than APS TBSs of more than 34%. Additionally, it was observed that all investigated properties increased significantly after thermal ageing. It was related to the formation of the porous layers, which occur at high temperature. Moreover, the results suggest that columnar structure increases thermal cycle durability compared to conventional lamellar APS TBCs. On the contrary, another research study [86] showed that the Young's modulus of APS also increases with the number of thermal cycles at 1150 °C, whereas the values of hardness gradually increases for the first 100 cycles, and then, decreases from 80 GPa to 75 GPa after 175 thermal cycles. In the study conducted by Wei et al. [87], the Young's modulus value of APS coating was changed with high-temperature exposure time. Once APS coating was detached from the Ni-based superalloy substrate, the elastic modulus was measured by using the ultrasonic method in the longitudinal and in transversal directions

before and after heating at 1400 °C for 1, 2, 5, 10 and 20 h. The results showed that the elastic modulus has a different value depending on the cross-section direction, which confirms an anisotropic character of the coating. In addition, elastic modulus determined for both directions rapidly increased with the high-temperature exposure time in the period less than 5 h, and then, decreased slowly. This was the effect of sintering process of the ceramic materials filled with microcracks and pores. This process was responsible for the shrinking or partial closing of defects after longer exposure at high temperature. Such features were confirmed by porosity and density tests. However, after 5 h of annealing, a new form of the micro-defects in the coating contributes to the decrease of the elastic modulus. Similar observations were presented by Tan et al. [88] for two YSZ coatings produced from different powder feedstock by using APS system on the steel substrate. The first type of coating was deposited with the fused and crushed powder (FC), and the second one with the hollow sphere powder (HOSP). After depositions, the coatings were detached from the substrate by polishing and subsequently examined. The Young's modulus was measured by the Resonant Ultrasound Spectroscopy (RUS) in different directions for both coatings before and after heat treatment at 1200 °C for 225 h. The results showed that the Young's modulus was higher after heat treatment for both coatings, and furthermore its value varied with the direction. In addition, materials with the HOSP coating exhibited a lower stiffness due to the larger scale of interlaminar pores and cracks. The authors also compared the anisotropic behaviour of the HVOF and APS nickel coatings at room temperature. The Ni-HVOF coating was characterized by a higher Young's modulus and a higher degree of elastic isotropy in comparison to the Ni-APS coating. Higher velocity during HVOF process guarantees the formation of uniform splats and layered structure with inhibited oxidation. The difference in the elastic isotropy was attributed to the increased number of cracks in the HVOF coating. However, the Ni-HVOF was less durable in the through-thickness direction even though it was still more isotropic than the Ni-APS.

Damage of the TBC coating can also occur due to insufficient adhesion between the BC and substrate. Since operation at elevated temperature leads to coating peeling or delamination, qualitative tests should be also carried out on the bond (adhesive or cohesive) at the interface between the bonding layer and the topcoat [89]. Kukla et al. [90] assessed the adhesion of the CVD-deposited aluminide coating on MAR 247 alloy. Its quality was verified by a scratch test under increasing force from 0 to 100 N and displacement of 10 mm. The results confirmed that the CVD-deposited coatings are able to withstand a critical force of 100 N during scratching without any spallation and breakdown of the layer.

The coated material typically exhibits an improved hardness of its surface. Liu et al. [91] clearly indicate that the mechanical properties of coating depend on the material and the deposition process used. Kukla et al. [90] reported that the hardness of MAR 247 with CVD aluminide coating gradually increased from the core material to the edge. The maximum hardness of the material was 650 HV0.05, while the core hardness was approximately 460HV0.05. Kopec et al. [80] obtained the maximum hardness of Inconel 740 with CVD aluminum layer, which occurred in the interdiffusion zone of 780 HV0.1. Hariharan et al. [92] investigated the impact of the thermal oxidation of coated Inconel 625 and Incoloy 800H superalloys on mechanical properties. In the research, YSZ coating with a thickness of 150 microns was used as the TC material with the BC material of NiCoAlY. The high-temperature oxidation testing of coated and uncoated specimens was performed at 1000 °C with molten salts: 70 g of sodium chloride and 30 g of potassium chloride in a muffle furnace for 8, 12 and 16 h, respectively. The heated specimens were used for mechanical testing (tensile and hardness tests). The tensile test conducted on uncoated and coated Inconel 625 and Incoloy 800H specimens exhibited that YSZ coating increased the yield strength and ultimate tensile strength regardless of the heating duration. Additionally, it was noted that the longer the heating time of specimens was, the higher difference of yield and tensile strength was obtained between the uncoated and YSZ coated specimens. Additionally, the hardness measurements revealed that the coating increases the mechanical properties of both alloys in question. It was concluded that YSZ-coated

materials after 16 h of annealing reduce hardness value more in the case of pure Incoloy 800H than Inconel 625. Li et al. [93] indicated that by means of the PS–PVD process, it is possible to deposit a YSZ coating of similar hardness value as the fully sintered zirconia ceramics. Furthermore, significantly higher hardness was observed for PS–PVD than for typical YSZ-coating deposited by using APS and EB-PVD systems. In the authors' latest work [94], the aluminization of Inconel 740 by using CVD process improved its fatigue response by around 100 MPa in the range of stress amplitude from 350 MPa to 650 MPa, as well as the hardness of the modified surface by a factor of 200%. The authors reported that the application of the aluminizing process can significantly improve the corrosion resistance of Inconel 740. It was concluded that the aluminizing process improves the heat resistance of Inconel 740 remarkably, and therefore it can be treated as a promising tool for material protection against high-temperature corrosion. The summary of the mechanical behaviour in relation to the deposition method and coating applied was presented in Table 2.

Table 2. Summary of the improved mechanical properties depending on the coating, deposition method and substrate applied.

Coating	Substrate	Method	Improved Properties	Reference
YSZ/ $Ni_{22}Co_{17}Cr_{12.5}Al_{0.6}Y$	C-263	APS	fatigue limit at high temperature	[77]
YSZ/ $Ni_{22}Co_{17}Cr_{12.5}Al_{0.6}Y$	C-263	APS	creep at 550–800 °C	[78]
zirconia-based/ NiCoCrAlYHf	DD6 Single Crystal Superalloy	EB-PVD/ arc ion plating	fatigue limit at high temperature	[79]
NiAl	MAR 247	CVD	fatigue limit at high temperature	[80]
Y-PSZ	-	APS	Young's module at high temperature	[87]
YSZ	-	APS	Young's module at high temperature	[88]
Ni	-	HVOF	Young's module at high temperature	[88]
NiAl	MAR 247	CVD	hardness	[90]
YSZ/NiCoAlY	Inconel 625	APS	tensile strength, yield strength, hardness: after heating at 1000 °C in the atmosphere of sodium and potassium chloride molten salts	[92]
YSZ/NiCoAlY	Incoloy 800H	APS	hardness: after heating at 1000 °C in the atmosphere of sodium and potassium chloride molten salts	[92]
YSZ	-	PS–PVD	hardness	[93]
NiAl	Inconel 740	CVD	fatigue, hardness, hot temperature corrosion	[94]

5. Conclusions and Future Trends

The characteristics of the most extensive materials used for thermal barrier coatings and deposition methods have been presented. It can be observed that most of the papers considered in this review are focused on the improvement of the particular property, including oxidation resistance, hardness, and mechanical behaviors. It should be emphasized, however, that the components protected with thermal barrier coatings operate under extreme conditions and in aggressive environments; thus, they are subjected to the combination of excessive loadings and oxidation. Hence, the coatings deposited on the substrate material, ideally whole components, should be subjected to the service loads under working conditions to simulate their real mechanical response in order to increase the reliability of the study performed. One should mention that the specific tests, either corrosion or mechanical, should not be performed on the coating only since its interaction with the substrate material should be investigated as well. The coating itself may have outstanding wear properties or be extremely resistant to oxidation; however, if it will not be adhered enough to the substrate, then its application will not possible. Thus, it is recommended to perform more studies which will focus on the actual interaction between the coating and substrate material subjected to loading under high temperature to assess the applicability of new methods or materials.

The direction of future investigations is proposed with a special emphasis on novel coating materials to provide oxidation-resistant and highly durable components. Nowadays, the vast majority of high-temperature components are based on nickel alloys, due to their high durability and standardized technology. Nevertheless, further improvements, such as structure or surface modification or industrialization of 3D printing, are mandatory to meet the requirements of the continuously expanding thermal barrier coatings market [95]. Based on the trends observed in the industry [96,97], it is estimated that the global thermal barrier coatings, market valued at USD 15.97 billion in 2021, are expected to grow at a compound annual growth rate (CAGR) of 4.6% during the forecast period of 2022–2030. It was reported [96] that the main damage mechanisms responsible for TBC failure are wear and corrosion. The deposition of hard-faced barrier coatings has been proposed as a useful approach to minimize the occurrence of such phenomena. Among conventionally used deposition methods, HVOF spraying was found as one of the most effective. On the other hand, the flame spraying can also be applied to form WC-based barrier coatings on nickel substrates. One should mention the applicability of plasma-transfer arc (PTA) welding in the mining and oil and gas industry. The thick tungsten carbide overlaying barrier coatings obtained during such a process improve the durability of protected components significantly. As reported in the recent literature [98], deposition techniques with non-line-of-sight capabilities in combination with columnar structures (SPS, PS–PVD) appear to be attractive for the application of TBCs, with special dedication for complex shaped parts. On the other hand, double-/multilayer coatings made of novel thermally stable materials combined with tough YSZ used directly on the bond coat will probably be the most reliable approach for high-temperature applications [98].

Author Contributions: Conceptualization, M.K.; methodology, I.B.; formal analysis, I.B. and M.K.; investigation, I.B.; resources, M.K.; data curation, I.B. and D.K.; writing—original draft preparation, I.B. and M.K.; writing—review and editing, C.S. and Z.L.K.; visualization, I.B. and D.K.; supervision, M.K. and Z.L.K.; project administration, M.K.; funding acquisition, M.K. and C.S. All authors have read and agreed to the published version of the manuscript.

Institutional Review Board Statement: Not applicable.

Informed Consent Statement: Not applicable.

Data Availability Statement: Not applicable.

Conflicts of Interest: The authors declare no conflict of interest.

References

1. Pavlenko, D.; Dvirnyk, Y.; Przysowa, R. Advanced materials and technologies for compressor blades of small turbofan engines. *IOP Conf. Ser. Mater. Sci. Eng.* **2021**, *1024*, 012061. [CrossRef]
2. Sahith, M.; Giridhara, G.; Kumar, S.R. Development and analysis of thermal barrier coatings on gas turbine blades—A Review. *Mater. Today Proc.* **2018**, *5*, 2746–2751. [CrossRef]
3. Szczepankowski, A.; Przysowa, R. Thermal degradation of turbine components in a military turbofan. *Eng. Fail. Anal.* **2022**, *134*, 106088. [CrossRef]
4. Przysowa, R. Blade Vibration Monitoring in a Low-Pressure Steam Turbine. In Proceedings of the ASME Turbo Expo 2018: Turbomachinery Technical Conference and Exposition, Oslo, Norway, 11–15 June 2018; Ceramics; Controls, Diagnostics, and Instrumentation; Education; Manufacturing Materials and Metallurgy. ASME: New York, NY, USA, 2018; Volume 6, p. V006T05A025.
5. Chellaganesh, D.; Khan, M.A.; Jappes, J.T.W. Thermal barrier coatings for high temperature applications—A short review. *Mater. Today Proc.* **2021**, *45*, 1529–1534. [CrossRef]
6. Naik, S. Basic Aspects of Gas Turbine Heat Transfer. In *Heat Exchangers*; Murshed, S.M.S., Lopes, M.M., Eds.; IntechOpen: Rijeka, Croatia, 2017; pp. 111–143.
7. Zhang, X.; Deng, Z.; Li, H.; Mao, J.; Deng, C.; Deng, C.; Niu, S.; Chen, W.; Song, J.; Fan, J.; et al. Al_2O_3-modified PS-PVD 7YSZ thermal barrier coatings for advanced gas-turbine engines. *npj Mater. Degrad.* **2020**, *4*, 31. [CrossRef]
8. Szczepankowski, A.; Przysowa, R.; Perczynski, J.; Kułaszka, A. Health and Durability of Protective and Thermal Barrier Coatings Monitored in Service by Visual Inspection. *Coatings* **2022**, *12*, 624. [CrossRef]
9. Moskal, G. Thermal barrier coatings: Characteristics of microstructure and properties, generation and directions of development of bond. *J. Achiev. Mater. Manuf.* **2009**, *37*, 323–331.
10. Bonaquist, D.; Feuerstein, A.; Buchakjian, L.; Brooks, P. *The Role of Thermal Barrier Coating in Maximizing Gas Turbine Engine Efciency and Lowering CO_2 Emissions*; Praxair Techology, Inc.: Danbury, CT, USA, 2017.
11. Bakan, E.; Vaßen, R. Ceramic Top coats of Plasma-Sprayed Thermal Barrier Coatings: Materials, Processes, and Properties. *J. Therm. Spray Technol.* **2017**, *26*, 992–1010. [CrossRef]
12. Falcón, J.C.P.; Echeverría, A.; Afonso, C.R.M.; Carrullo, J.C.Z.; Borrás, V.A. Microstructure assessment at high temperature in NiCoCrAlY overlay coating obtained by laser metal deposition. *J. Mater. Res. Technol.* **2019**, *8*, 1761–1772. [CrossRef]
13. Hu, Y.; Cai, C.; Wang, Y.; Yu, H.; Zhou, Y.; Zhou, G. YSZ/NiCrAlY interface oxidation of APS thermal barrier coatings. *Corros. Sci.* **2018**, *142*, 22–30. [CrossRef]
14. Daroonparvar, M.; Yajid, M.A.M.; Yusof, N.M.; Farahany, S.; Hussain, M.S.; Bakhsheshi-Rad, H.R.; Valefi, Z.; Abdolahi, A. Improvement of thermally grown oxide layer in thermal barrier coating systems with nano alumina as third layer. *Trans. Nonferrous Met. Soc. China* **2013**, *23*, 1322–1333. [CrossRef]
15. Deevi, S.C. Advanced intermetallic iron aluminide coatings for high temperature applications. *Prog. Mater. Sci.* **2021**, *118*, 100769. [CrossRef]
16. Senderowski, C.; Cinca, N.; Dosta, S.; Cano, I.G.; Guilemany, J.M. The Effect of Hot Treatment on Composition and Microstructure of HVOF Iron Aluminide Coatings in Na_2SO_4 Molten Salts. *J. Therm. Spray Technol.* **2019**, *28*, 1492–1510. [CrossRef]
17. Senderowski, C.; Panas, A.J.; Fikus, B.; Zasada, D.; Kopec, M.; Korytchenko, K.V. Effects of Heat and Momentum Gain Differentiation during Gas Detonation Spraying of FeAl Powder Particles into the Water. *Materials* **2021**, *14*, 7443. [CrossRef]
18. Panas, A.J.; Senderowski, C.; Fikus, B. Thermophysical properties of multiphase Fe-Al intermetallic-oxide ceramic coatings deposited by gas detonation spraying. *Thermochim. Acta* **2019**, *676*, 164–171. [CrossRef]
19. Pawlowski, A.; Czeppe, T.; Major, L.; Senderowski, C. Structure Morphology of Fe-Al Coating Detonation Sprayed onto Carbon Steel Substrate. *Arch. Metall. Mater.* **2009**, *54*, 783–788.
20. Pawlowski, A.; Senderowski, C.; Wolczynski, W.; Morgiel, J.; Major, L. Detonation Deposited Fe-Al Coatings Part II: Transmission Electron Microscopy of Interlayers and Fe-Al Intermetallic Coating Detonation Sprayed onto the 045 Steel Substrate. *Arch. Metall. Mater.* **2011**, *56*, 71–79. [CrossRef]
21. Senderowski, C.; Vigilianska, N.; Burlachenko, O.; Grishchenko, O.; Murashov, A.; Stepanyuk, S. Effect of APS Spraying Parameters on the Microstructure Formation of Fe_3Al Intermetallics Coatings Using Mechanochemically Synthesized Nanocrystalline Fe-Al Powders. *Materials* **2023**, *16*, 1669. [CrossRef]
22. Lencová, K.; Frank Netrvalová, M.; Vostřák, M.; Lukáč, F.; Mušálek, R.; Česánek, Z.; Houdková, Š. Hot Corrosion Behavior of TWAS and HVOF NiCr-Based Coatings in Molten Salt. *Materials* **2023**, *16*, 1712. [CrossRef]
23. Reinshagen, J.H.; Sikka, V.K. Thermal spraying of selected aluminides. In *Thermal Spray Coatings: Properties, Processes and Applications*; Bernecki, T.F., Ed.; ASM International: Materials Park, OH, USA, 1991.
24. Al-Taie, I.; Brigham, R.J.; Lafreniere, Y. High temperature alloys and thermal spray coatings for energy conversion. In Proceedings of the 2nd International Conference on Heat Resistant Materials, Gatlinburg, TN, USA, 11–14 September 1995; Natesan, K., Ganesan, P., Lai, G., Eds.; ASM International: Materials Park, OH, USA, 1995; pp. 437–444.
25. Senderowski, C.; Bojar, Z. Gas detonation spray forming of Fe–Al coatings in the presence of interlayer. *Surf. Coat. Technol.* **2008**, *202*, 3538. [CrossRef]
26. Kumar, N.; Gupta, M.; Mack, D.E.; Mauer, G.; Vaßen, R. Columnar Thermal Barrier Coatings Produced by Different Thermal Spray Processes. *J. Therm. Spray Technol.* **2021**, *30*, 1437–1452. [CrossRef]

27. Feuerstein, A.; Knapp, J.; Taylor, T.; Ashary, A.; Bolcavage, A.; Hitchman, N. Technical and Economical Aspects of Current Thermal Barrier Coating Systems for Gas Turbine Engines by Thermal Spray and EBPVD: A Review. *J. Therm. Spray Technol.* **2008**, *17*, 199–213. [CrossRef]

28. Ruys, A.J.; Sutton, B.A. Metal-ceramic functionally graded materials (FGMs). In *Metal-Reinforced Ceramics*; Ruys, A.J., Ed.; Woodhead Publishing: Cambridge, UK, 2021; pp. 327–359.

29. Juhasz, J.A.; Best, S.M. Surface modification of biomaterials by calcium phosphate deposition. In *Surface Modification of Biomaterials*; Williams, R., Ed.; Woodhead Publishing: Cambridge, UK, 2011; pp. 143–169.

30. Wang, M. Composite coatings for implants and tissue engineering scaffolds. In *Biomedical Composites*, 2nd ed.; Ambrosio, L., Ed.; Woodhead Publishing: Cambridge, UK, 2010; pp. 127–177.

31. Jordan, E.H.; Jiang, C.; Gell, M. The Solution Precursor Plasma Spray (SPPS) Process: A Review with Energy Considerations. *J. Therm. Spray Technol.* **2015**, *24*, 1153–1165. [CrossRef]

32. Mauer, G.; Jarligo, M.O.; Mack, D.E.; Vaßen, R. Plasma-Sprayed Thermal Barrier Coatings: New Materials, Processing Issues, and Solutions. *J. Therm. Spray Technol.* **2013**, *22*, 646–658. [CrossRef]

33. Devasia, R.; Painuly, A.; Devapal, D.; Sreejith, K.J. Continuous fiber reinforced ceramic matrix composites. In *Fiber Reinforced Composites*; Joseph, K., Oksman, K., George, G., Wilson, R., Appukuttan, S., Eds.; Woodhead Publishing: Cambridge, UK, 2021; pp. 669–751.

34. Bakan, E.; Mack, D.E.; Mauer, G.; Vaßen, R.; Lamon, J.; Padture, N.P. High-temperature materials for power generation in gas turbines. In *Advanced Ceramics for Energy Conversion and Storage*; Guillon, O., Ed.; Elsevier: Amsterdam, The Netherlands, 2020; pp. 3–62.

35. Fikus, B.; Senderowski, C.; Panas, A.J. Modeling of Dynamics and Thermal History of Fe40Al Intermetallic Powder Particles Under Gas Detonation Spraying Using Propane-Air Mixture. *J. Therm. Spray Technol.* **2019**, *28*, 346–358. [CrossRef]

36. Ramadan, K.; Butler, P.B. Analysis of gas flow evolution and shock wave decay in detonation thermal spraying systems. *J. Therm. Spray Technol.* **2004**, *13*, 239–247. [CrossRef]

37. Chrostek, T. Tribological wear of Fe-Al coatings applied by gas detonation spraying. *Tech. Sci.* **2021**, *24*, 245–256. [CrossRef]

38. Astakhov, E.A. Controlling the properties of detonation-sprayed coatings: Major aspects. *Powder Metall. Met. Ceram.* **2008**, *47*, 70–79. [CrossRef]

39. El-Eskandarany, M.S. Utilization of ball-milled powders for surface protective coating. In *Mechanical Alloying*, 3rd ed.; El-Eskandarany, M.S., Ed.; William Andrew Publishing: Norwich, NY, USA, 2020; pp. 309–334.

40. Raza, A.; Ahmad, F.; Badri, T.M.; Raza, M.R.; Malik, K. An Influence of Oxygen Flow Rate and Spray Distance on the Porosity of HVOF Coating and Its Effects on Corrosion—A Review. *Materials* **2022**, *15*, 6329. [CrossRef]

41. Weman, K. (Ed.) Surface cladding and hardfacing methods. In *Welding Processes Handbook*, 2nd ed.; Woodhead Publishing: Cambridge, UK, 2012; pp. 151–156.

42. El-Eskandarany, M.S. (Ed.) Introduction. In *Mechanical Alloying*, 2nd ed.; William Andrew Publishing: Norwich, NY, USA, 2015; pp. 1–12.

43. Coppens, K.; Ferraris, E. Chemical Vapor Deposition (CVD). In *CIRP Encyclopedia of Production Engineering*; Chatti, S., Laperrière, L., Reinhart, G., Tolio, T., Eds.; Springer: Berlin/Heidelberg, Germany, 2019; pp. 239–243.

44. Mbam, S.O.; Nwonu, S.E.; Orelaja, O.A.; Nwigwe, U.S.; Gou, X.-F. Thin-film coating; historical evolution, conventional deposition technologies, stress-state micro/nano-level measurement/models and prospects projection: A critical review. *Mater. Res. Express* **2019**, *6*, 122001. [CrossRef]

45. Qiu, S.-Y.; Wu, C.-W.; Huang, C.-G.; Ma, Y.; Guo, H.-B. Microstructure Dependence of Effective Thermal Conductivity of EB-PVD TBCs. *Materials* **2021**, *14*, 1838. [CrossRef]

46. Mehboob, G.; Liu, M.-J.; Xu, T.; Hussain, S.; Mehboob, G.; Tahir, A. A review on failure mechanism of thermal barrier coatings and strategies to extend their lifetime. *Ceram. Int.* **2020**, *46*, 8497–8521. [CrossRef]

47. Avci, A.; Eker, A.A.; Eker, B. Microstructure and Oxidation Behavior of Atmospheric Plasma-Sprayed Thermal Barrier Coatings, Exergetic. In *Energetic and Environmental Dimensions*; Dincer, I., Colpan, C.O., Kizilkan, O., Eds.; Academic Press: Cambridge, MA, USA, 2018; pp. 793–814.

48. Shen, Z.; He, L.; Xu, Z.; Mu, R.; Huang, G. LZC/YSZ DCL TBCs by EB-PVD: Microstructure, low thermal conductivity and high thermal cycling life. *J. Eur. Ceram. Soc.* **2019**, *39*, 1443–1450. [CrossRef]

49. Bernard, B.; Quet, A.; Bianchi, L.; Joulia, A.; Malié, A.; Schick, V.; Rémy, B. Thermal insulation properties of YSZ coatings: Suspension Plasma Spraying (SPS) versus Electron Beam Physical Vapor Deposition (EB-PVD) and Atmospheric Plasma Spraying (APS). *Surf. Coat. Technol.* **2017**, *318*, 122–128. [CrossRef]

50. Mao, J.; Liu, M.; Deng, Z.; Wen, K.; Deng, C.; Yang, K.; Chen, Z. Coating deposition regularity depended on orientation difference in PS-PVD plasma jet. *CJA* **2020**, *33*, 3460–3468. [CrossRef]

51. Doll, G.L.; Mensah, B.A.; Mohseni, H.; Scharf, T.W. Chemical Vapor Deposition and Atomic Layer Deposition of Coatings for Mechanical Applications. *J. Therm. Spray Technol.* **2009**, *19*, 510–516. [CrossRef]

52. Geremew, T. Thin Film Deposition and Characterization Techniques. *J. 3D Print. Appl.* **2022**, *1*, 1–24.

53. Mauer, G.; Vaßen, R. Coatings with Columnar Microstructures for Thermal Barrier Applications. *Adv. Eng. Mater.* **2020**, *22*, 1900988. [CrossRef]

54. von Niessen, K.; Gindrat, M. Plasma Spray-PVD: A New Thermal Spray Process to Deposit Out of the Vapor Phase. *J. Therm. Spray Technol.* **2011**, *20*, 736–743. [CrossRef]

55. Mahade, S.; Curry, N.; Björklund, S.; Markocsan, N.; Nylén, P.; Vaßen, R. Functional performance of $Gd_2Zr_2O_7$/YSZ multi-layered thermal barrier coatings deposited by suspension plasma spray. *Surf. Coat. Technol.* **2017**, *318*, 208–216. [CrossRef]

56. Ganvir, A.; Joshi, S.; Markocsan, N.; Vassen, R. Tailoring columnar microstructure of axial suspension plasma sprayed TBCs for superior thermal shock performance. *Mater. Des.* **2018**, *144*, 192–208. [CrossRef]

57. Kukla, D.; Kopec, M.; Wang, K.; Senderowski, C.; Kowalewski, Z.L. Nondestructive Methodology for Identification of Local Discontinuities in Aluminide Layer-Coated MAR 247 during Its Fatigue Performance. *Materials* **2021**, *14*, 3824. [CrossRef] [PubMed]

58. Huang, Y.; Peng, X. The promoted formation of an α-Al_2O_3 scale on a nickel aluminide with surface Cr_2O_3 particles. *Corros. Sci.* **2016**, *112*, 226–232. [CrossRef]

59. Doleker, K.M.; Odabas, O.; Ozgurluk, Y.; Askerov, H.; Karaoglanli, A.C. Effect of high temperature oxidation on Inconel 718 and Inconel 718/YSZ/$Gd_2Zr_2O_7$. *Mater. Res. Express* **2019**, *6*, 086456. [CrossRef]

60. He, J. Advanced MCrAlY alloys with doubled TBC lifetime. *Surf. Coat. Technol.* **2022**, *448*, 128931. [CrossRef]

61. Taylor, T.A.; Walsh, P.N. Thermal expansion of MCrAlY alloys. *Surf. Coat. Technol.* **2004**, *177–178*, 24–31. [CrossRef]

62. Bergholz, J.; Pint, B.A.; Unocic, K.A.; Vaßen, R. Fabrication of oxide dispersion strengthened bond coats with low Al_2O_3 content. *J. Therm. Spray Technol.* **2017**, *26*, 868–879. [CrossRef]

63. Vorkötter, C.; Hagen, S.P.; Pintsuk, G.; Mack, D.E.; Virtanen, S.; Guillon, O.; Vaßen, R. Oxide dispersion strengthened bond coats with higher alumina content: Oxidation resistance and influence on thermal barrier coating lifetime. *Oxid. Met.* **2019**, *92*, 167–194. [CrossRef]

64. Wells, J.; Chapman, N.; Sumner, J.; Walker, P. The Use of APS Thermal Barrier Coatings in Corrosive Environments. *Oxid. Met.* **2017**, *88*, 97–108. [CrossRef]

65. Gupta, M.; Markocsan, N.; Li, X.H.; Östergren, L. Influence of Bondcoat Spray Process on Lifetime of Suspension Plasma-Sprayed Thermal Barrier Coatings. *J. Therm. Spray Technol.* **2018**, *27*, 84–97. [CrossRef]

66. Curry, N.; Tang, Z.; Markocsan, N.; Nylén, P. Influence of Bond Coat Surface Roughness on the Structure of Axial Suspension Plasma Spray Thermal Barrier Coatings—Thermal and Lifetime Performance. *Surf. Coat. Technol.* **2015**, *268*, 15–23. [CrossRef]

67. Bernard, B.; Quet, A.; Bianchi, L.; Schick, V.; Joulia, A.; Malié, A.; Rémy, B. Effect of Suspension Plasma-Sprayed YSZ Columnar Microstructure and Bond Coat Surface Preparation on Thermal Barrier Coating Properties. *J. Therm. Spray Technol.* **2017**, *26*, 1025–1037. [CrossRef]

68. Sokołowski, P.; Pawłowski, L.; Dietrich, D.; Lampke, T.; Jech, D. Advanced Microscopic Study of Suspension Plasma-Sprayed Zirconia Coatings with Different Microstructures. *J. Therm. Spray Technol.* **2016**, *25*, 94–104. [CrossRef]

69. Seo, D.; Ogawa, K.; Shoji, T.; Murata, S. Effect of Particle Size Distribution on Isothermal Oxidation Characteristics of Plasma Sprayed CoNi- and CoCrAlY Coatings. *J. Therm. Spray Technol.* **2007**, *16*, 954–966. [CrossRef]

70. Padture, N.P.; Gell, M.; Jorda, E.H. Thermal Barrier Coatings for Gas-Turbine Engine Application. *Science* **2002**, *296*, 280–284. [CrossRef] [PubMed]

71. Parchovianský, M.; Parchovianská, I.; Hanzel, O.; Netriová, Z.; Pakseresht, A. Phase Evaluation, Mechanical Properties and Thermal Behavior of Hot-Pressed LC-YSZ Composites for TBC Applications. *Materials* **2022**, *15*, 2839. [CrossRef]

72. Wang, L.; Yang, J.; Ni, J.; Liu, C.; Zhong, X.; Shao, F.; Zhao, H.; Tao, S.; Wang, Y. Influence of cracks in APS-TBCs on stress around TGO during thermal cycling: A numerical simulation study. *Surf. Coat. Technol.* **2016**, *285*, 98–112. [CrossRef]

73. Schlichting, K.W.; Padture, N.P.; Klemens, P.G. Thermal conductivity of dense and porous yttria-stabilized zirconia. *J. Mater. Sci.* **2001**, *36*, 3003–3010. [CrossRef]

74. Jang, B.K.; Matsubara, H. Influence of porosity on hardness and Young's modulus of nanoporous EB-PVD TBCs by nanoindentation. *Mater. Lett.* **2005**, *5*, 3462–3466. [CrossRef]

75. Wee, S.; Do, J.; Kim, K.; Lee, C.; Seok, C.; Choi, B.-G.; Choi, Y.; Kim, W. Review on Mechanical Thermal Properties of Superalloys and Thermal Barrier Coating Used in Gas Turbines. *Appl. Sci.* **2020**, *10*, 5476. [CrossRef]

76. Musalek, R.; Kovarik, O.; Medricky, J.; Curry, N.; Bjorklund, S.; Nylen, P. Fatigue Testing of TBC on Structural Steel by Cyclic Bending. *J. Therm. Spray Technol.* **2015**, *24*, 168–174. [CrossRef]

77. Ray, A.K.; Dwarakadasa, E.S.; Das, D.K.; Ranganath, V.R.; Goswami, B.; Sahu, J.K.; Whittenberger, J.D. Fatigue behavior of a thermal barrier coated superalloy at 800 °C. *Mater. Sci. Eng. A* **2007**, *448*, 294–298. [CrossRef]

78. Ray, A.K.; Das, D.K.; Venkataraman, B.; Roy, P.K.; Goswami, B.; Roy, N.; Das, S.K.; Parida, N.; Tarafder, S.; Chaudhuri, S.; et al. Characterization of rupture and fatigue resistance of TBC superalloy for combustion liners. *Mater. Sci. Eng. A* **2005**, *405*, 194–200. [CrossRef]

79. Dong, J.; Li, J.; Mu, R.; Tian, H. Fatigue Behavior of Thermal Barrier Coated DD6 Single Crystal Superalloy at 900 °C. In *Physics and Engineering of Metallic Materials*; Han, Y., Ed.; Springer: Singapore, 2019; Volume 217, pp. 347–356.

80. Kopec, M.; Kukla, D.; Yuan, X.; Rejmer, W.; Kowalewski, Z.L.; Senderowski, C. Aluminide Thermal Barrier Coating for High Temperature Performance of MAR 247 Nickel Based Superalloy. *Coatings* **2021**, *11*, 48. [CrossRef]

81. Zhu, W.; Wu, Q.; Yang, L.; Zho, Y.C. In situ characterization of high temperature elastic modulus and fracture toughness in air plasma sprayed thermal barrier coatings under bending by using digital image correlation. *Ceram. Int.* **2020**, *46*, 18526–18533. [CrossRef]

82. Zhu, Q.; He, W.; Zhu, J.; Zhou, Y.; Chen, L. Investigation on interfacial fracture toughness of plasma-sprayed TBCs using a three-point bending method. *Surf. Coat. Technol.* **2018**, *353*, 75–83. [CrossRef]

83. Evans, A.G.; Mumm, D.R.; Hutchinson, J.W.; Meier, G.H.; Pettit, F.S. Mechanisms controlling the durability of thermal barrier coatings. *Prog. Mater. Sci.* **2001**, *46*, 505–553. [CrossRef]

84. Chen, Y.; Zhang, X.; Zhao, X.; Markocsan, N.; Nylén, P.; Xiao, P. Measurements of elastic modulus and fracture toughness of an air plasma sprayed thermal barrier coating using micro-cantilever bending. *Surf. Coat. Technol.* **2019**, *374*, 12–20. [CrossRef]

85. Yamazaki, Y.; Morikawa, M.; Hamaguchi, T.; Habu, Y.; Ohide, Y.; Takagi, K. Relationship between the mechanical properties and structure of a suspension plasma-sprayed thermal barrier coating with columnar microstructure. *Surf. Coat. Technol.* **2022**, *439*, 128430. [CrossRef]

86. Mao, W.G.; Luo, J.M.; Dai, C.Y.; Shen, Y.G. Effect of heat treatment on deformation and mechanical properties of 8 mol% yttria-stabilized zirconia by Berkovich nanoindentation. *Appl. Surf. Sci.* **2015**, *338*, 92–98. [CrossRef]

87. Wei, Q.; Zhu, J.; Chen, W. Anisotropic Mechanical Properties of Plasma-Sprayed Thermal Barrier Coatings at High Temperature Determined by Ultrasonic Method. *J. Therm. Spray Technol.* **2016**, *25*, 605–612. [CrossRef]

88. Tan, Y.; Shyam, A.; Choi, W.B.; Lara-Curzio, E.; Sampath, S. Anisotropic elastic properties of thermal spray coatings determined via resonant ultrasound spectroscopy. *Acta Mater.* **2010**, *58*, 5305–5315. [CrossRef]

89. Nayak, H.; Krishnamurthy, N.; Shailesh, R.A. Development and Adhesion Strength of Plasma-Sprayed Thermal Barrier Coating on the Cast Iron Substrate. *Int. J. Integr. Eng.* **2021**, *13*, 47–59.

90. Kukla, D.; Kopec, M.; Kowalewski, Z.L.; Politis, D.J.; Jóźwiak, S.; Senderowski, C. Thermal Barrier Stability and Wear Behavior of CVD Deposited Aluminide Coatings for MAR 247 Nickel Superalloy. *Materials* **2020**, *13*, 3863. [CrossRef]

91. Liu, S.H.; Trelles, J.P.; Murphy, A.B.; He, W.T.; Shi, J.; Li, S.; Li, C.J.; Li, C.X.; Guo, H.B. Low-pressure plasma-induced physical vapor deposition of advanced thermal barrier coatings: Microstructures, modelling and mechanisms. *Mater. Today Phys.* **2021**, *21*, 100481. [CrossRef]

92. Hariharan, M.K.; Anderson, A.; Praveenkumar, T.R.; Mosisa, E. Investigation on Hot Corrosion Behaviour of Inconel 625 and Incoloy 800H Superalloys with YSZ-Thermal Barrier Coating Under High-Temperature Environment for Bioreactor Applications. *J. Nanomater.* **2022**, *2022*, 5861391.

93. Li, J.; Huang, H.; Ma, T.; Eguchi, K.; Yoshida, T. Twin-Structured Yttria-Stabilized t' Zirconia Coatings Deposited by Plasma Spray Physical Vapor Deposition: Microstructure and Mechanical Properties. *J. Am. Ceram. Soc.* **2007**, *90*, 603–607. [CrossRef]

94. Barwinska, I.; Kopec, M.; Kukla, D.; Łaźińska, M.; Sitek, R.; Kowalewski, Z.L. Effect of Aluminizing on the Fatigue and High-Temperature Corrosion Resistance of Inconel 740 Nickel Alloy. *JOM* **2023**, *75*, 1–13. [CrossRef]

95. Mondal, K.; Nuñez, L.; Downey, C.M.; van Rooyen, I.J. Recent advances in the thermal barrier coatings for extreme environments. *Mater. Sci. Technol.* **2021**, *4*, 208–210. [CrossRef]

96. *Thermal Barrier Coatings Market Share, Size, Trends, Industry Analysis Report, Segment Forecast, 2022–2030*; POLARIS: Medina, MN, USA, 2022; Available online: https://www.polarismarketresearch.com/industry-analysis/thermal-barrier-coatings-tbc-market (accessed on 13 April 2023).

97. Thermal Barrier Coatings Market—Growth, Trends, COVID-19 Impact, and Forecasts (2023–2028). Available online: https://www.researchandmarkets.com/reports/4897094/thermal-barrier-coatings-market-growth (accessed on 13 April 2023).

98. Vaßen, R.; Bakan, E.; Mack, D.E.; Guillon, O. A Perspective on Thermally Sprayed Thermal Barrier Coatings: Current Status and Trends. *J. Therm. Spray Technol.* **2022**, *31*, 685–698. [CrossRef]